Original Article
https://doi.org/10.5115/acb.2018.51.2.105
pISSN 2093-3665 eISSN 2093-3673
Anatomy & Cell Biology acb

CD57 (Leu-7, HNK-1) immunoreactivity seen in thin arteries in the human fetal lung

Satoshi Ishizuka[1], Zhe Wu Jin[2], Masahito Yamamoto[1], Gen Murakami[1,3], Takeshi Takayama[4], Katsuhiko Hayashi[4], Shin-ichi Abe[1]

[1]Department of Anatomy, Tokyo Dental College, Tokyo, Japan, [2]Department of Anatomy, Wuxi Medical School, Jiangnan University, Wuxi, China, [3]Division of Internal Medicine, Iwamizawa Asuka Hospital, Iwamizawa, [4]Department of Dentistry, Jikei University School of Medicine, Tokyo, Japan

Abstract: CD57 (synonyms: Leu-7, HNK-1) is a well-known marker of nerve elements including the conductive system of the heart, as well as natural killer cells. In lung specimens from 12 human fetuses at 10–34 weeks of gestation, we have found incidentally that segmental, subsegmental, and more peripheral arteries strongly expressed CD57. Capillaries near developing alveoli were often or sometimes positive. The CD57-positive tissue elements within intrapulmonary arteries seemed to be the endothelium, internal elastic lamina, and smooth muscle layer, which corresponded to tissue positive for a DAKO antibody reactive with smooth muscle actin we used. However, the lobar artery and pulmonary arterial trunk as well as bronchial arteries were negative. Likewise, arteries in and along any abdominal viscera, as well as the heart, thymus, and thyroid, did not express CD57. Thus, the lung-specific CD57 reactivity was not connected with either of an endodermal- or a branchial arch-origin. CD57 antigen is a sugar chain characterized by a sulfated glucuronic acid residue that is likely to exist in some glycosphingolipids. Therefore, a chemical affinity or an interaction might exist between CD57-positive arterioles and glycosphingolipids originating from alveoli, resulting in acceleration of capillary budding to make contact with the alveolar wall. CD57 might therefore be a functional marker of the developing air-blood interface that characterizes the fetal lung at the canalicular stage.

Key words: CD57, Leu-7, HNK-1, Lung, Human fetus

Received December 15, 2017; Revised February 5, 2018; Accepted February 16, 2018

Introduction

The CD57 antigen corresponds to an epitope named "HNK-1 sugar chain" characterized by a sulfated glucuronic acid residue. It plays a critical role in neural development [1]. In early studies, HNK-1 was known to be an antibody useful for identification of migrating neural crest cells [2, 3] as well as the conductive system of heart [4, 5]. Later, when HNK-1 was used more extensively in research, hematologists focused on the antigen "Leu-7," which was useful for discriminating natural killer cells from CD8-positive suppressive lymphocytes [6]: Leu-7 also corresponds to CD57. Therefore, CD57 has often been used in different two fields of science: neuroscience and hematology.

During observations of intrapulmonary nerves and ganglia, we incidentally found CD57-positive arteries in the human fetal lung (10–34 weeks of gestation), even though we were using CD57 simply as a neuronal marker. At this fetal stage, the canalicular phase of lung development occurs, where peripheral arterioles give off numerous capillaries to provide an air-blood interface [7]. Consequently, the aim of this preliminary report was to characterize the expression of CD57 specifically in fetal intrapulmonary arteries.

Corresponding author:
Masahito Yamamoto
Department of Anatomy, Tokyo Dental College, 2-9-18 Misaki-cho, Chiyoda-ku, Tokyo 101-0061, Japan
Tel: +81-3-6380-9592, Fax: +81-3-6380-9664, E-mail: yamamotomasahito@tdc.ac.jp

Materials and Methods

This study was performed in accordance with the principles of the Declaration of Helsinki 1995 (as revised in 2013). We observed semiserial sagittal sections of (1) seven Chinese specimens at 10–16 weeks (crown-rump length [CRL], 50–125 mm) and (2) five Japanese specimens at 30–34 weeks (CRL, 250–290 mm). Primarily, these sections had been prepared for a study of intrapulmonary nerves and ganglia (not published), but the presence of CD57-positive arteries had been found incidentally.

The seven Chinese fetal specimens were donated by the families concerned to the Department of Anatomy, Yanbian University Medical College, Yanji, China, up to 2016 and their use for research was approved by the university ethics committee in Yanji (No. BS-13-35). The fetuses had been obtained by induced abortion, after which each mother had been orally informed by an obstetrician at the college teaching hospital

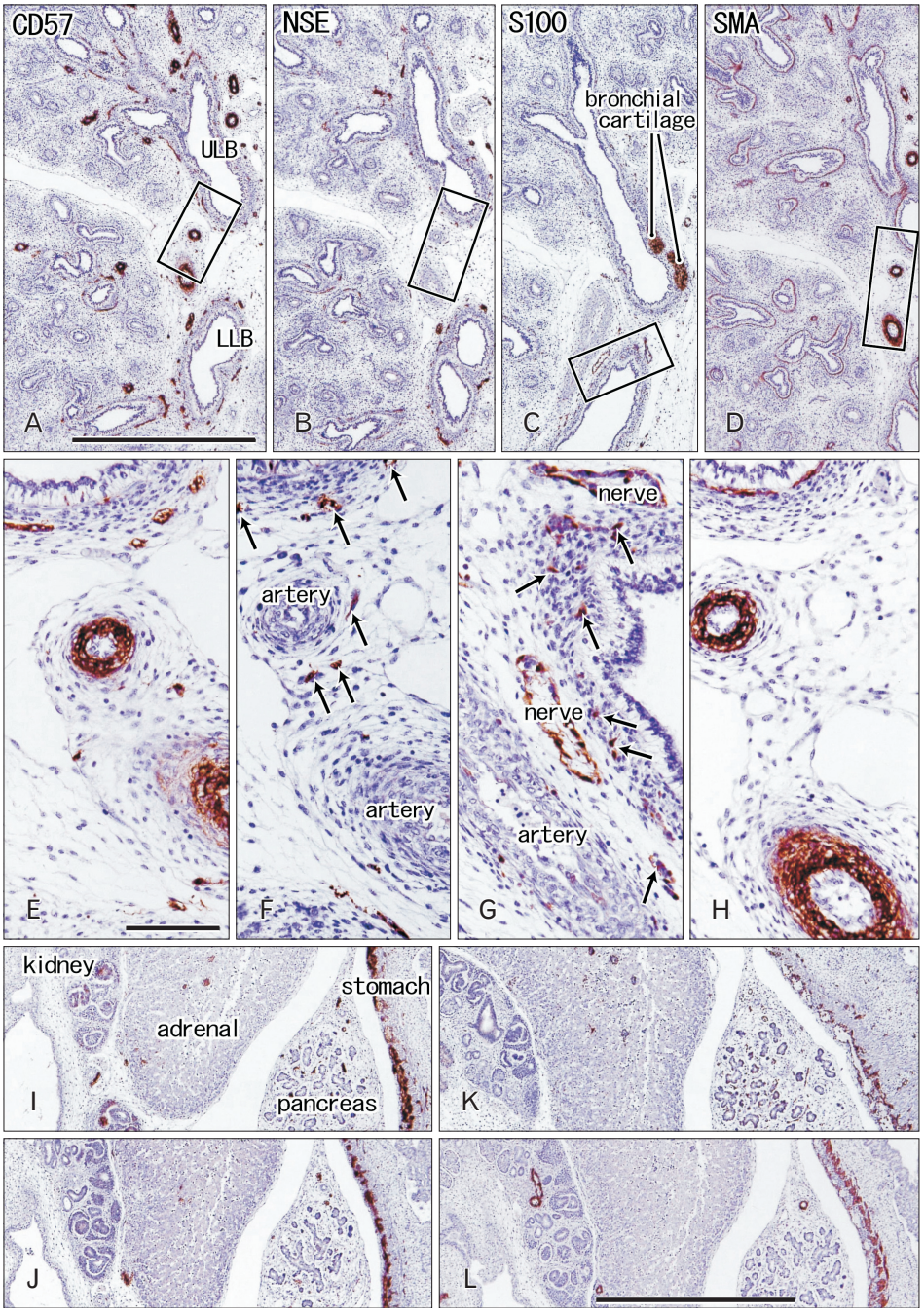

Fig. 1. Immunohistochemistry of the lung, kidney, adrenal, pancreas, and stomach in sections from a specimen at 10 weeks (50-mm crown-rump length). Sagittal sections. Panels A–H show immunostaining of the left lung (A and E, CD57; B and F, neuron-specific enolase [NSE]; C and G, S100; D and H, smooth muscle actin [SMA]), while panels I–L show that of the kidney, adrenal, pancreas and stomach. Panels E–H are higher-magnification views of the squares in panels A–D, respectively. Arrows in panels F and G indicate positive nerve elements. Panels I (CD57), J (NSE), K (S100), or L (SMA) displays the same section as shown in panel A, B, C, or D. Panels A–D, panels E–H, and panels I–L were prepared at the same magnification, respectively. ULB, upper lobar bronchus; LLB, lower lobar bronchus. Scale bars=1 mm (A, L), 0.1 mm (E).

of the possibility of donating the fetus for research; no attempt had been made to actively encourage the donation. After agreement had been obtained from the mother, the fetus was assigned a specimen number and stored in 10% w/w neutral formalin solution for more than 1 month. Because of specimen number randomization, there was no possibility of contacting the family at a later date. The trunk samples were decalcified by incubation at 4°C in a 0.5-mol/L EDTA (pH 7.5) decalcifying solution (Decalcifying Solution B, Wako, Tokyo, Japan) for 3–5 days, depending on the size of the sample. After routine procedures for paraffin embedded histology, the specimens were sliced sagittally or horizontally at 20–50 μm intervals depending on their sizes, and then cut into sections 5 μm thick.

The five Japanese specimens were part of the collection kept at the Department of Anatomy, Akita University, Akita, Japan. They had been donated to the Department by the families concerned during 1975–1985 and preserved in 10% w/w neutral formalin solution for more than 30 years. The available data were limited to the date of donation and the number of gestational weeks, but there was no documentary record of the family name, the name of the obstetrician(s), the hospital,

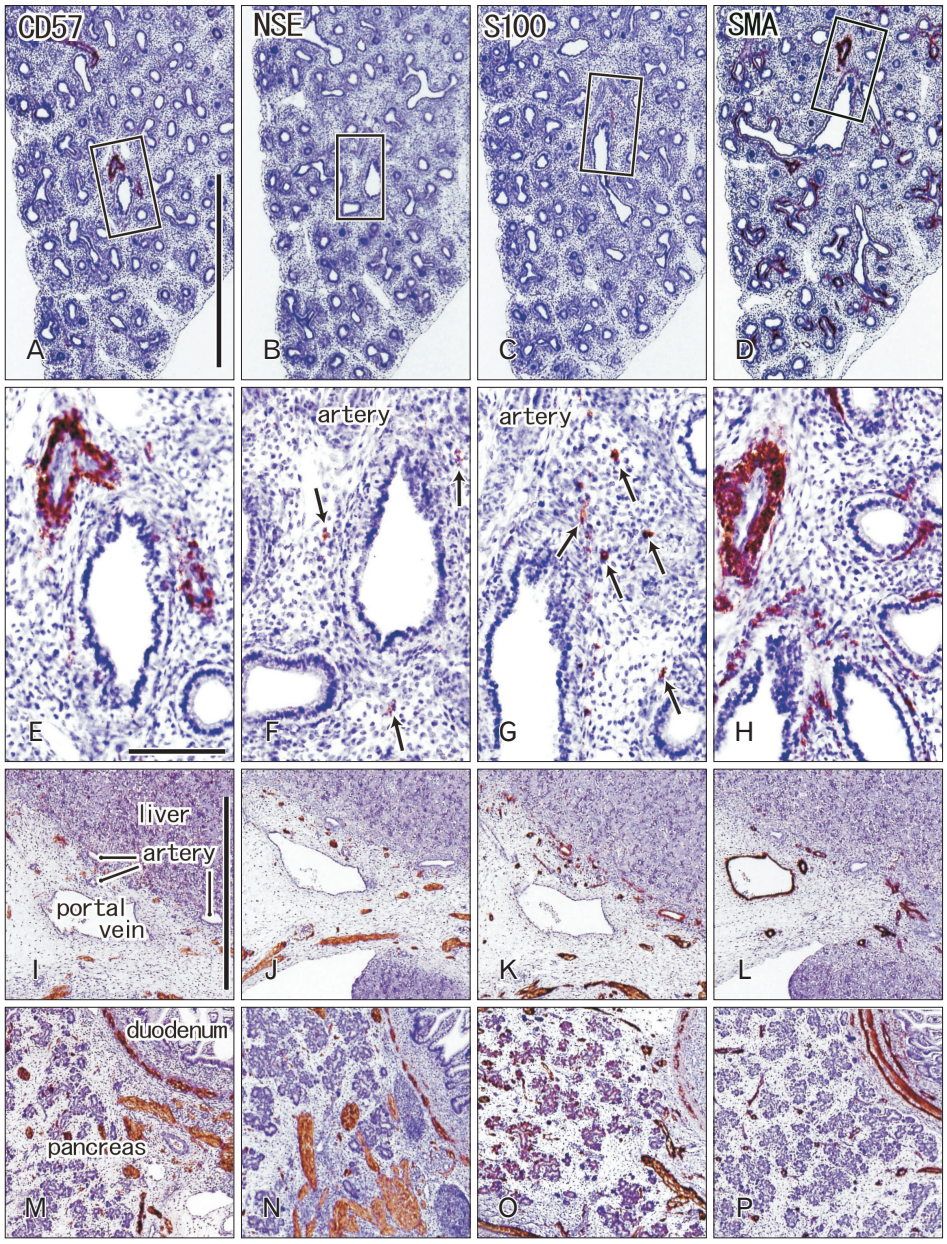

Fig. 2. Immunohistochemistry of the lung, liver, pancreas, and duodenum in sections from a specimen at 15 weeks (110 mm crown-rump length). Sagittal sections. Panels A–H show immunostaining of the right lung lower lobe (A and E, CD57; B and F, neuron-specific enolase [NSE]; C and G, S100; D and H, smooth muscle actin [SMA]). Panels E–H are higher-magnification views of the squares in panels A–D, respectively. Arrows in panels F and G indicate positive nerve elements. Panels I–L show that of the hilar portion of the liver including hepatic arteries and portal vein. Panels M–O show that of the pancreas and duodenum. Panels I and M (CD57), panels J and N (NSE), panels K and O (S100), or panels L and P (SMA) display the same section as shown in panel A, B, C or D. Panels A–D, panels E–H, and panels I–P were prepared at the same magnification, respectively. Scale bars=1 mm (A, I), 0.1 mm (E).

https://doi.org/10.5115/acb.2018.51.2.105

or the reason for abortion. Use for research was approved by the university ethics committee in Akita (No. 1428). After removal of the thoracic viscera, we prepared 5 large paraffin blocks containing the whole heart as well as parts of the lung, thymus, esophagus and diaphragm. From each of the blocks, we prepared semiserial sagittal sections (5 μm in thickness) at intervals of 50-200 μm.

The primary antibodies used for immunohistochemistry were (1) purified mouse anti-human CD57 (dilution 1:30, clone HNK-1, BD Bioscience, San Jose, CA, USA), (2) mouse monoclonal anti-human neuron-specific enolase (NSE; dilution 1:200, Dako N1557, Dako, Glostrup, Denmark), (3) mouse monoclonal anti-human S100 protein (S100; 1:100, Z0311, Dako), and (4) mouse monoclonal anti-human α-smooth muscle actin (SMA; 1:100, M0760, Dako). Except for the S100 and SMA antibodies, antigen retrieval was performed using microwave treatment (500 W, 15 minutes, pH 6). The secondary antibody (incubation for 30 minutes;

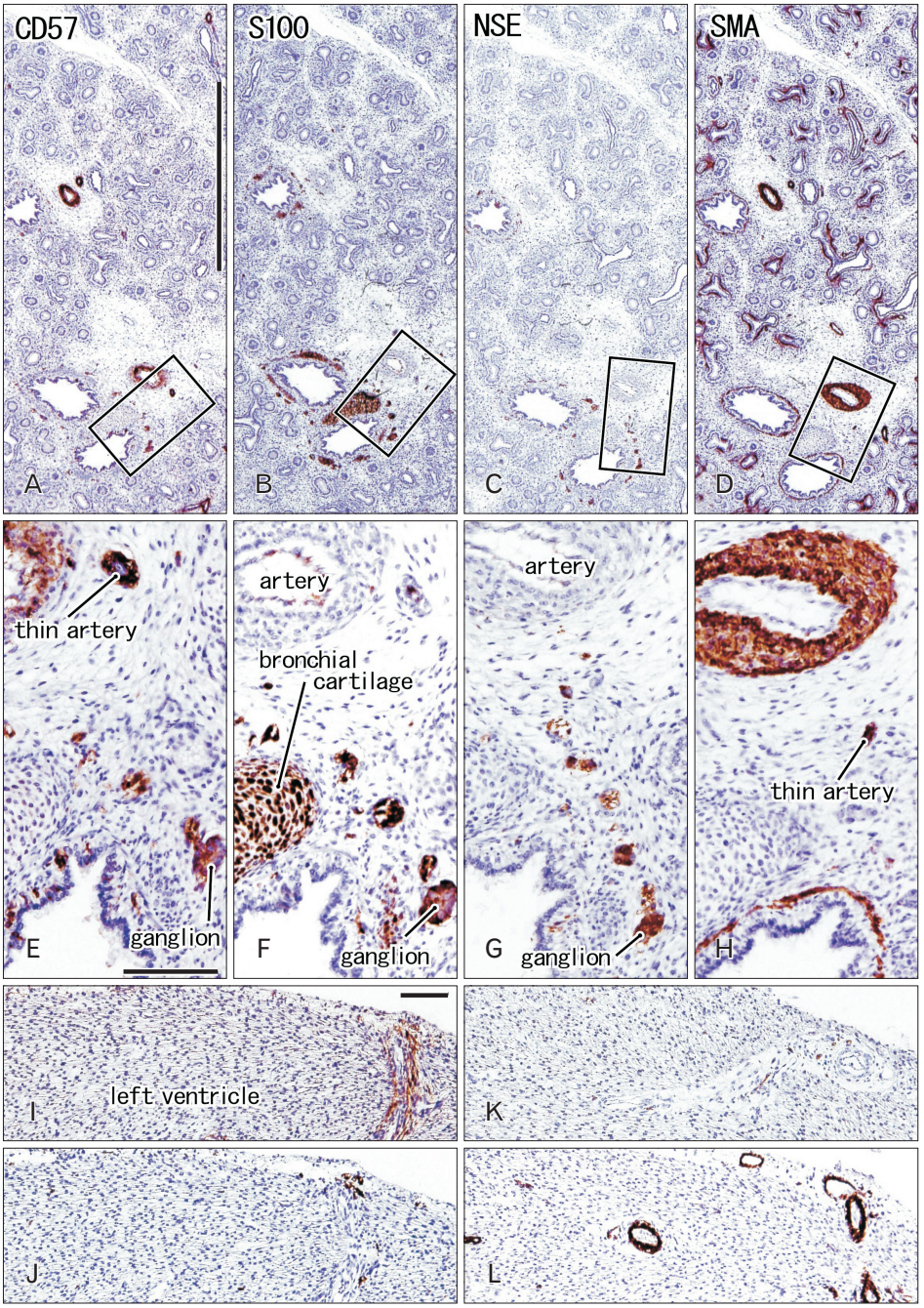

Fig. 3. Immunohistochemistry of the lung and heart in sections from a specimen at 16 weeks (125 mm crown-rump length). Horizontal sections. Panels A–H show immunostaining of the left lung lower lobe (A and E, CD57; B and F, S100; C and G, neuron-specific enolase [NSE]; D and H, smooth muscle actin [SMA]), while panels I–L show that of the left ventricular wall. Panels E–H are higher-magnification views of the squares in panels A–D, respectively. Panels A and B (or C and D) are adjacent sections. Panel I (CD57), panel J (S100), panel K (NSE), or panel L (SMA) displays the same section as shown in panel A, B, C, or D. Panels A–D, panels E–H, and panels I–L were prepared at the same magnification, respectively. Scale bars=1 mm (A, I), 0.1 mm (E).

dilution 1:1,000, Histofine Simple Stain Max-PO, Nichirei, Tokyo, Japan) was labeled with horseradish peroxidase (HRP), and antigen-antibody reactions were detected by the HRP-catalyzed reaction with diaminobenzidine (incubation for 3–5 minutes; Histofine Simple Stain DAB). All samples were counterstained with hematoxylin. Negative controls consisted of samples without the primary antibody. We had noted previously that the Dako anti-SMA antibody reacted strongly with the endothelium of arteries and veins [8, 9]. In addition, we also used mouse monoclonal anti-human CD8 (1:100, Dako N1592), but only non-specific staining was obtained, even in the thymus and lymph nodes of all the specimens we examined.

Results

Observations of the lung

The present mid-term specimens displayed a morphology in which the pseudoglandular and canalicular phased-bronchioles were mixed, while the late-stage specimens had reached the saccular phase but also contained abundant bronchioles at the earlier phases. In these lungs, CD57 immunoreactivity was positive in the endothelium as well as the smooth muscle layer of thin arteries less than 0.2 mm in diameter (Figs. 1–4). The arteries mostly corresponded to the segmental, subsegmental and more peripheral levels of the pulmonary arterial tree. The maximum thickness of the posi-

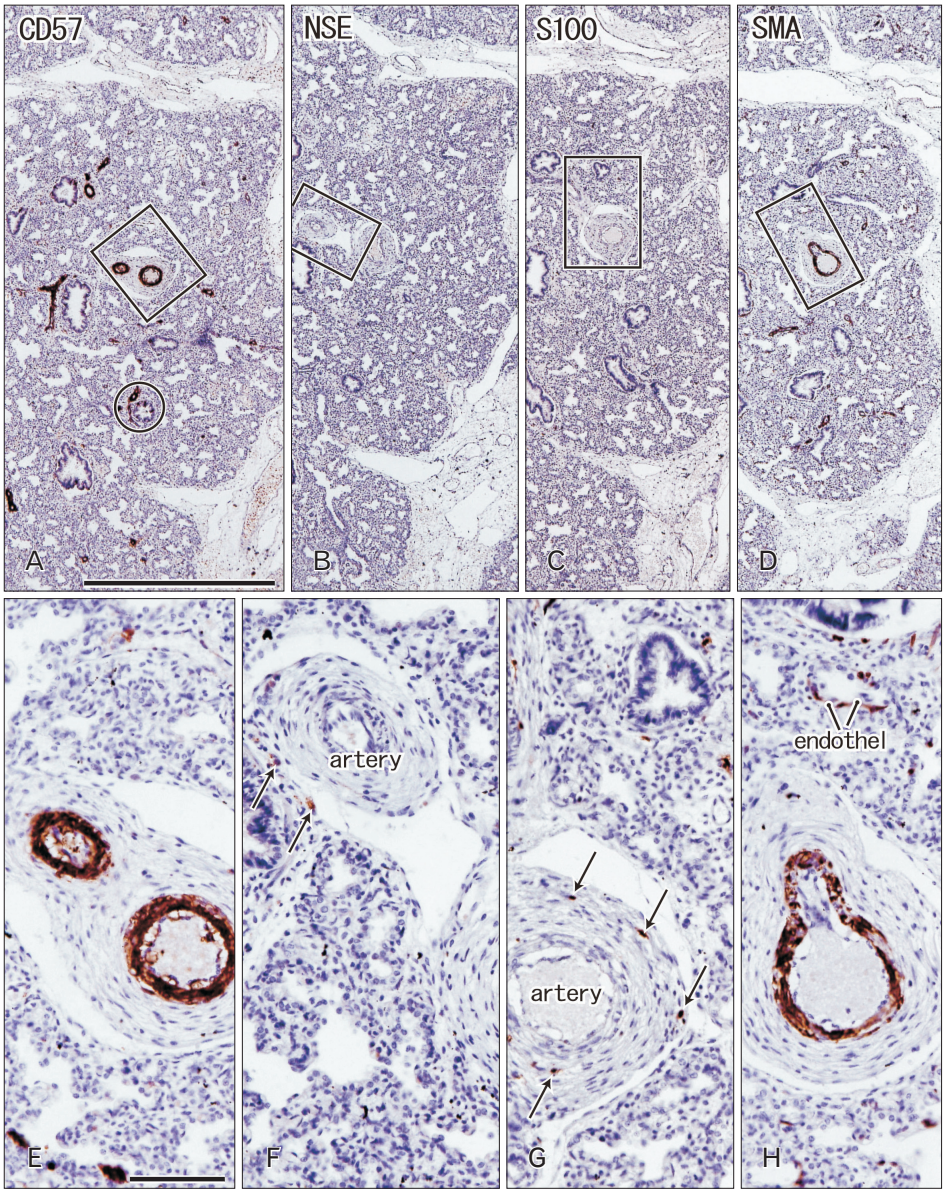

Fig. 4. Immunohistochemistry of the lung in sections from a specimen at 30 weeks (255 mm crown-rump length). Sagittal sections. Panels A–H show immunostaining of the right lung middle lobe (A and E, CD57; B and F, neuron-specific enolase [NSE]; C and G, S100; D and H, smooth muscle actin [SMA]). Panels E–H are higher-magnification views of the squares in panels A–D, respectively. Two circles in panel A are shown in Fig. 5 at higher magnification. Panels A–D and panels E–H were prepared at the same magnification, respectively. Arrows is panel F and G indicate positive nerve elements. Scale bars=1 mm (A), 0.1 mm (E).

https://doi.org/10.5115/acb.2018.51.2.105

tive arteries did not differ appreciably between the mid-term and late stages: 0.05–0.15 mm and 0.1–0.2 mm, respectively. In contrast, no immunoreactivity was seen in the pulmonary arterial trunk and lobar arteries as well as bronchial arteries along the primary bronchi. Any veins in and around the lung were also negative. In late-stage specimens (Fig. 4), arterioles much thinner than the subsegmental arteries also expressed CD57 strongly, but all capillaries near or adjacent to the alveoli were not positive (Fig. 5A–C).

CD57 expression was also found in nerves and ganglia along and around the arteries and bronchi. The CD57 immunoreactivity was found in NSE-positive and/or S100-positive structures, but the positive nerves tended to be more numerous than those positive for NSE or S100. In the specimens after 14 weeks, neuro-endocrine cells of the bronchus and bronchiole expressed CD57 strongly (Fig. 5D) and NSE weakly, but were negative for S100. SMA immunoreactivity was seen in the endothelium as well as the smooth muscle layer of arteries and arterioles. However, capillaries near or adjacent to alveoli were negative for SMA. In the bronchi, a thin layer beneath the columnar epithelium was SMA-positive (Figs. 1H, 2H, 3H): this layer had an appearance similar to that of an "intestinal muscularis mucosae" but most likely corresponded to the initial morphology of the bronchial smooth muscle layer. Overall, the CD57-positive tissue elements in intrapulmonary arteries corresponded to tissues that were reactive with the Dako antibody against SMA (Figs. 1E, H, 3E, H, 4E, H), i.e., (1) the arterial endothelium, (2) the internal elastic lamina that developed in the late stage, and (3) the smooth muscle layer.

Observations of other structures

The present sagittal sections contained the brain, spinal cord, trunk muscles and nerves as well as viscera other than the lung in the same sections: the thyroid, thymus, heart, esophagus, stomach, small intestine and colon, pancreas, liver, kidney, adrenal and testis. In all these viscera, arteries did not express CD57. The diameter of these negative arteries was

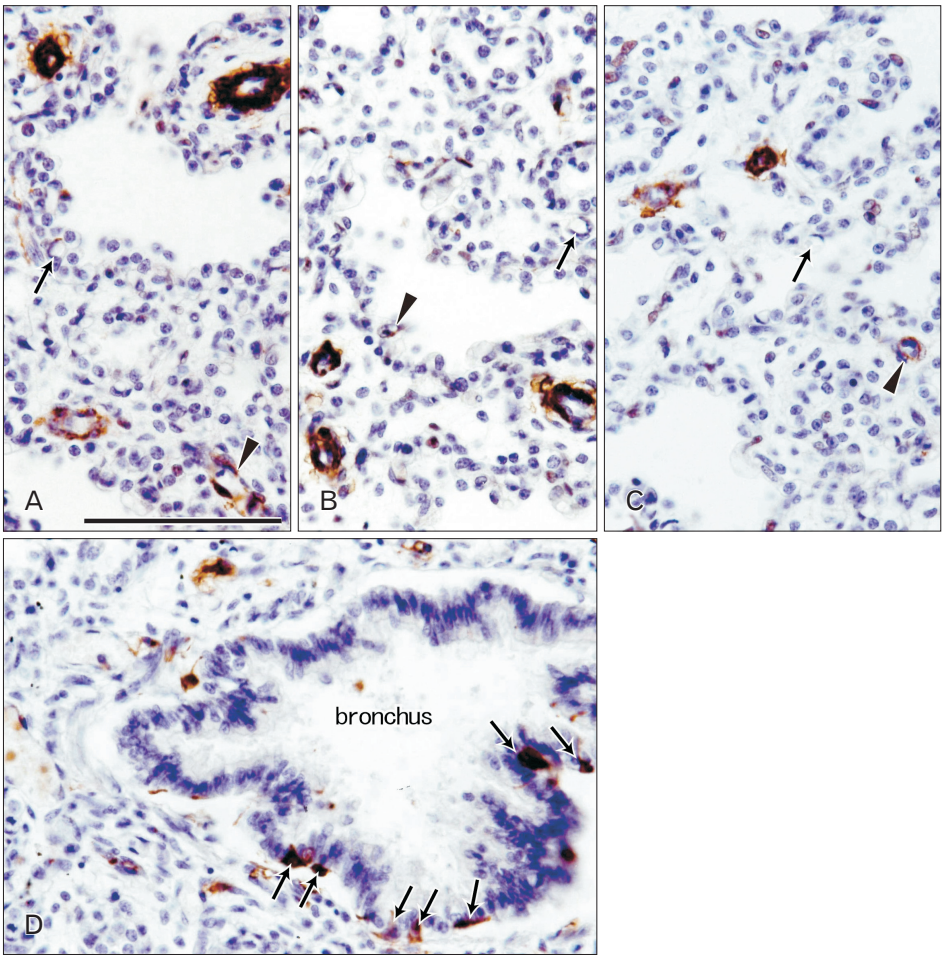

Fig. 5. CD57 reactivity in arterioles and capillaries near and adjacent to alveoli as well as in neuroendocrine cells of the bronchi. Sagittal sections. Panels A–C show peripheral alveolar areas in a specimen of 235 mm crown-rump length (CRL). Panel D displays a higher-magnification view of the circle in Fig. 4A (30 weeks; 255 mm CRL). Panels A–C contain both CD57-positive (arrowheads) and negative (arrows) capillaries. Arterioles are strongly positive. Panel D exhibits a subsegmental bronchus containing CD57-positive neuroendocrine cells (arrows). The other positive structures around the bronchus are supplying nerves: some of them to the bronchus. All panels were prepared at the same magnification. Scale bar=0.1 mm (A).

almost identical to the positive intrapulmonary arteries: i.e., Fig. 2A vs. Fig. 2I (same magnification); thin artery in Fig. 3E (×20 at objective lens) vs. Fig. 3I (×10 at objective lens). All nerves were positive for CD57 as well as NSE and S100 in the pancreas, stomach and intestines (Fig. 2M–O). In addition to the nerve elements, we found CD57 expression in some of the capsules surrounding the glomerulus in the renal cortex (Fig. 1I). SMA immunoreactivity was evident in hepatic arteries (Fig. 2L) and coronary arteries (Fig. 3L), but these arteries did not express CD57. Likewise, arteries in the kidney, adrenal, pancreas were positive for SMA but did not express CD57 (Fig. 1I, L). Nerves in and along the ventricular wall were strongly positive for CD57, but weakly positive for NSE and S100 (Fig. 3I, J). The acinus of the exocrine pancreas and the sublingual gland expressed S100 and/or NSE (Fig. 1). Finally, skeletal muscles as well as the brain and spinal cord did not contain CD57-positive arteries: these peripheral arteries were positive for SMA.

Discussion

This may be the first report of CD57 immunoreactivity in intrapulmonary arteries. However, the most striking feature noted in the present study was the total lack of CD57 expression in other arteries. Thus, the expression seemed to be lung-specific. Since CD57 expression was evident even in thin arterioles, antigenicity seemed to be well maintained in the long-preserved, late stage fetuses. At the beginning of this study, we speculated that arteries of endodermal or branchial arch origin would express CD57, but the thymus and thyroid did not contain such positive arteries. Since positivity was seen not only in mid-term but also late-stage fetuses, it was likely present at birth. In pulmonary arteries at the segmental and subsegmental levels, the maximum thickness did not differ appreciably between stages; it was almost 2 times thicker in the late stage. Thus, we were unable to rule out the possibility that the reactivity was dependent on arterial diameter: an increased thickness would make the expression weak and the lobar artery was too thick to be positive. Nevertheless, negativity of CD57 was evident in tissues other than the lung when compared with arteries of the same or similar thickness. In addition, although non-nerve tissues in the pancreas and salivary gland express CD57, S100, and/or NSE, the positive tissues did not include any arteries [10-13].

CD57 seems to play various roles in differentiation of the neural crest and lymphocytes (see the "Introduction"). In the same context, the antibody is available as a marker of inactive or senescent T lymphocytes [14] as well as of specific lymphocytes involved in the initial stage of atherosclerosis [15, 16] and myocardial infarction [17]. Unfortunately, we failed CD8 immunostaining of the present materials (see the final sentence of "Materials and Methods"). The alveolus as well as the arterial endothelium contain glycosphingolipids: part of the HNK-1 sugar chain is likely to be contained in the latter [18]. Although CD57 reactivity was weak in capillaries near and adjacent to alveoli, some form of chemical affinity or interaction might be present between CD57-postive arterioles and glycosphingolipids contained in proliferating and growing alveoli, resulting in accelerated development of numerous and frequent capillary buds making contact with the alveolar wall. CD57 might thus be a functional marker of the developing air-blood interface of the fetal lung at the canalicular stage. If arterial CD57 is connected with differentiation of the air-blood interface, its expression would be maintained up to almost 1 year after birth, as the proliferation of alveoli continues [7].

References

1. Kleene R, Schachner M. Glycans and neural cell interactions. Nat Rev Neurosci 2004;5:195-208.
2. Bronner-Fraser M. Analysis of the early stages of trunk neural crest migration in avian embryos using monoclonal antibody HNK-1. Dev Biol 1986;115:44-55.
3. Verberne ME, Gittenberger-de Groot AC, Poelmann RE. Lineage and development of the parasympathetic nervous system of the embryonic chick heart. Anat Embryol (Berl) 1998;198:171-84.
4. Ikeda T, Iwasaki K, Shimokawa I, Sakai H, Ito H, Matsuo T. Leu-7 immunoreactivity in human and rat embryonic hearts, with special reference to the development of the conduction tissue. Anat Embryol (Berl) 1990;182:553-62.
5. Aoyama N, Tamaki H, Kikawada R, Yamashina S. Development of the conduction system in the rat heart as determined by Leu-7 (HNK-1) immunohistochemistry and computer graphics reconstruction. Lab Invest 1995;72:355-66.
6. Vassiliadou N, Bulmer JN. Immunohistochemical evidence for increased numbers of 'classic' CD57+ natural killer cells in the endometrium of women suffering spontaneous early pregnancy loss. Hum Reprod 1996;11:1569-74.
7. O'Rahilly R, Müller F. Human embryology and teratology. 2nd ed. New York: Wiley-Liss; 1996. p.265-71.
8. Hayashi S, Murakami G, Ohtsuka A, Itoh M, Nakano T, Fukuzawa Y. Connective tissue configuration in the human liver hilar region with special reference to the liver capsule and vascular sheath. J Hepatobiliary Pancreat Surg 2008;15:640-7.
9. Miyake N, Hayashi S, Kawase T, Cho BH, Murakami G, Fujimiya

https://doi.org/10.5115/acb.2018.51.2.105

M, Kitano H. Fetal anatomy of the human carotid sheath and structures in and around it. Anat Rec (Hoboken) 2010;293:438-45.
10. Haimoto H, Hosoda S, Kato K. Differential distribution of immunoreactive S100-alpha and S100-beta proteins in normal nonnervous human tissues. Lab Invest 1987;57:489-98.
11. Matsunou H, Konishi F. Papillary-cystic neoplasm of the pancreas: a clinicopathologic study concerning the tumor aging and malignancy of nine cases. Cancer 1990;65:283-91.
12. Yantiss RK, Chang HK, Farraye FA, Compton CC, Odze RD. Prevalence and prognostic significance of acinar cell differentiation in pancreatic endocrine tumors. Am J Surg Pathol 2002;26:893-901.
13. Kawamoto A, Kitamura K, Yamamoto M, Murakami G, Abe S, Katori Y. Morphological differences in innervation between mucous glands and serous glands: a quantitative histological study using the sublingual glands of elderly humans. Acta Otolaryngol 2015;135:942-9.
14. Kaplan RC, Sinclair E, Landay AL, Lurain N, Sharrett AR, Gange SJ, Xue X, Parrinello CM, Hunt P, Deeks SG, Hodis HN. T cell activation predicts carotid artery stiffness among HIV-infected women. Atherosclerosis 2011;217:207-13.
15. Schumacher H, Kaiser E, Schnabel PA, Sykora J, Eckstein HH, Allenberg JR. Immunophenotypic characterisation of carotid plaque: increased amount of inflammatory cells as an independent predictor for ischaemic symptoms. Eur J Vasc Endovasc Surg 2001;21:494-501.
16. Winchester R, Giles JT, Nativ S, Downer K, Zhang HZ, Bag-Ozbek A, Zartoshti A, Bokhari S, Bathon JM. Association of elevations of specific T cell and monocyte subpopulations in rheumatoid arthritis with subclinical coronary artery atherosclerosis. Arthritis Rheumatol 2016;68:92-102.
17. Yu HT, Youn JC, Lee J, Park S, Chi HS, Lee J, Choi C, Park S, Choi D, Ha JW, Shin EC. Characterization of CD8(+)CD57(+) T cells in patients with acute myocardial infarction. Cell Mol Immunol 2015;12:466-73.
18. Duvar S, Peter-Katalinić J, Hanisch FG, Müthing J. Isolation and structural characterization of glycosphingolipids of in vitro propagated bovine aortic endothelial cells. Glycobiology 1997;7:1099-109.